PRAMANA
— journal of
physics

Vol. ??, No. ?
Month Year
pp. 1–11

Multiparticle azimuthal correlations

N BORGHINI
Service de Physique Théorique, CP225, Université Libre de Bruxelles, 1050 Brussels, Belgium

P M DINH and J-Y OLLITRAULT
Service de Physique Théorique, CEA-Saclay, 91191 Gif-sur-Yvette cedex, France

Abstract. First observations of elliptic flow in Au-Au collisions at RHIC have been interpreted as evidence that the colliding system reaches thermal equilibrium. We discuss some of the arguments leading to this conclusion and show that a more accurate analysis is needed, which the standard flow analysis may not provide. We then present a new method of flow analysis, based on a systematic study of multiparticle azimuthal correlations. This method allows one to test quantitatively the collective behaviour of the interacting system. It has recently been applied by the STAR Collaboration at RHIC.

Keywords. heavy ion collisions, elliptic flow, correlations, cumulants

PACS Nos 25.75.Ld 25.75.Gz

1. Introduction

One of the first results that came from Au-Au collisions at the Relativistic Heavy Ion Collider (RHIC) at Brookhaven was the observation that elliptic flow is by a factor of 2 larger than at SPS [1]. This was interpreted as an evidence that thermal equilibrium in ultrarelativistic heavy ion collisions had been achieved for the first time at RHIC [2]. This issue of thermalisation is crucial: it is a prerequisite to the formation of a quark-gluon plasma in these collisions, since this new state of matter is defined assuming thermal equilibrium. But it is a non-trivial issue: although we know that many strongly interacting particles are formed in a heavy ion collision at RHIC, the system is expanding so rapidly that it cannot be described as a static thermal bath; thermal equilibrium is at best achieved locally, if the mean free path of particles is much smaller than a typical size of the system.

One usually distinguishes several types of thermal equilibria: equilibrium with respect to inelastic collisions which constrains the relative abundances of particle species [3] ("chemical" equilibrium). On the other hand, equilibrium with respect to elastic collisions constrains momentum distributions, and implies in particular that they are isotropic in the local rest frame. This is the "kinetic" equilibrium, on which we concentrate here. Kinetic equilibrium itself has two aspects. One is the equilibration between longitudinal and transverse degrees of freedom, i.e., the implication that in the local rest frame, longitudinal and transverse momenta are of the same order of magnitude. This aspect of thermalisation can be

discussed from first principles at the partonic level [4], and there is now a vast literature on this subject [5]. But experimental signatures deal in fact rather with equilibration among the two transverse degrees of freedom. Due to the high Lorentz contraction at ultrarelativistic energies, the typical transverse size is much larger than the longitudinal size, so that this "transverse equilibrium" is probably easier to achieve than "longitudinal-transverse equilibrium".

Elliptic flow is a phenomenon which results from final state interactions: if there are no mutual collisions between the produced particles, elliptic flow simply vanishes. For this reason, it is widely believed to be the most sensitive probe of transverse kinetic equilibrium [6].

In Sec. 2., we recall the definition of elliptic flow and explain the mechanism producing elliptic flow at ultrarelativistic energies. We then discuss the centrality dependence of elliptic flow, as well as the transverse momentum dependence of elliptic flow of identified particles. We shall see that measurements of elliptic flow may provide a clean signature of transverse thermalisation. In Sec. 3., we discuss the methods used to analyse elliptic flow. We show that "standard" methods are unable to provide reliable measurements at ultrarelativistic energies: "nonflow" correlations, which are neglected in the standard analysis, may bias the observations, in particular the centrality dependence of elliptic flow. We then present a new method recently developed to overcome the limitations of the standard analysis, based on a cumulant expansion of multiparticle azimuthal correlations. Application of this method to STAR data will be presented, and the issue of thermalisation will be discussed in this context.

2. Elliptic flow: a signature of transverse thermalisation

2.1 Directed and elliptic flow: definitions

In a non-central nucleus-nucleus collision, the impact parameter defines a reference direction in the transverse plane. One usually calls "reaction plane" the plane spanned by the impact parameter and the collision axis. It turns out that azimuthal angles of outgoing particles are most often correlated to this reference direction. This is the phenomenon of *anisotropic flow*. If ϕ denotes the azimuthal angle of a particle with respect to the reaction plane (see Fig. 1), such a correlation means that the ϕ distribution is not flat. The latter is usually expanded in Fourier series [7]:

$$\frac{dN}{d\phi} \propto 1 + 2\sum_{n=1}^{\infty} v_n \cos(n\phi), \tag{1}$$

where terms proportional to $\sin(n\phi)$ vanish due to the $\phi \to -\phi$ symmetry. The Fourier coefficients v_n characterize the strength of anisotropic flow:

$$v_n = \langle \cos(n\phi) \rangle = \left\langle e^{in\phi} \right\rangle, \tag{2}$$

where brackets denote a statistical average. The first two Fourier coefficients v_1 and v_2 are usually called "directed flow" and "elliptic flow", and have been measured at various colliding energies, from below 50 MeV per nucleon up to RHIC energies. [8]

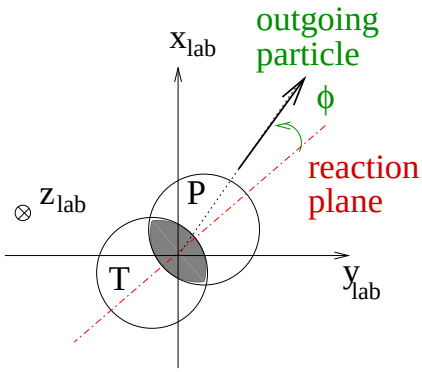

Figure 1. Nucleus-nucleus collisions viewed in the transverse plane. $x_{\rm lab}$ and $y_{\rm lab}$ are fixed directions in the laboratory system. The dash-dotted line is the direction of impact parameter, or reaction plane.

This phenomenon is of crucial importance for the following reason: if the nucleus-nucleus collision were a mere superposition of independent nucleon-nucleon collisions, the ϕ distribution would be flat: a pair of colliding nucleons does not see the impact parameter of the whole nucleus-nucleus collision. For this reason, anisotropies in the ϕ distribution must result from final state interactions between the produced particles. This is illustrated below, where we discuss a mechanism that produces elliptic flow at ultrarelativistic energies.

2.2 The physics of elliptic flow

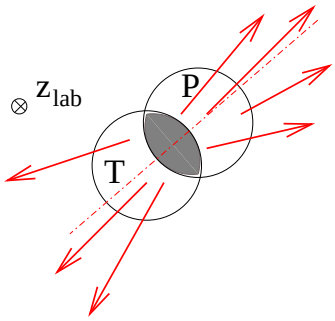

Figure 2. Typical directions of outgoing particles at ultrarelativistic energies.

At ultrarelativistic energies, the azimuthal anisotropy is dominated by elliptic flow, and v_2 is positive. This can be easily understood. A large number of particles are created in an almond-shaped region, represented by the shaded area in Fig. 2. Interactions between these particles result in a pressure which is highest at the center of the almond, and zero outside. At a given point, the resulting force per unit volume is opposite to the pressure gradient. Now, the gradient is larger along the smaller direction of the almond, which is

precisely the direction of the reaction plane. Thus one expects stronger collective motion in the direction of the reaction plane (i.e., with $\cos(2\phi) > 0$) than in the perpendicular direction (with $\cos(2\phi) < 0$). This results in a positive value of v_2 defined by Eq. (2), which was predicted in Ref. [6] and later observed at the top AGS energy [9] and at SPS [10].

2.3 Centrality dependence of elliptic flow

Hydrodynamical models, which assume thermal equilibrium throughout the evolution of the system, are able to provide stable, quantitative predictions for this effect. Indeed, elliptic flow is essentially determined by two ingredients, which we discuss separately.

The first ingredient is the shape of the almond in Fig. 2, i.e., the distribution of energy in the transverse plane, which is well controlled theoretically. The momentum anisotropy v_2 calculated in hydro models is proportional to the anisotropy of the almond (defined as the relative difference between the smaller and the larger dimension of the almond) [6]. When plotted as a function of centrality (as estimated from the total charged multiplicity produced in the collision), this anisotropy decreases linearly, and so does the elliptic flow v_2 in hydrodynamic models. This is illustrated by recent calculations displayed in Fig. 3. For the most central collisions, the almond becomes a circle and v_2 vanishes by symmetry. What is less obvious is that the maximum value of v_2 occurs for impact parameters as large as 12 fm or even higher.

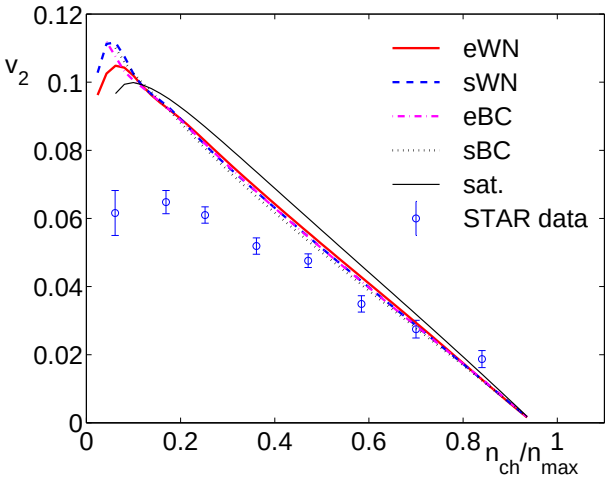

Figure 3. Elliptic flow as a function of centrality for a Au-Au collision at RHIC. The curves are predictions of a hydrodynamic model, from Ref. [11], for various choices of initial conditions. The data are taken from Ref. [1].

The second essential ingredient in v_2 is pressure (resulting from final state interactions), which converts the anisotropy of the initial distribution into anisotropy of the momentum distribution. Pressure is included in hydro models through an equation of state, which is an input of the model. The thermodynamical quantity which matters here, rather than the pressure itself, is the velocity of sound, $c_s \equiv \sqrt{dP/d\epsilon}$ (with ϵ the total energy density),

which determines the pressure gradient. For a given value of c_s, v_2 decreases linearly with centrality, as discussed above, but the slope (i.e., the absolute magnitude of v_2 for a given centrality) depends on c_s. As one could expect intuitively, a higher value of c_s ("hard" equation of state) produces a higher value of v_2. With a softer equation of state than the one chosen in the calculations displayed in Fig. 3, one could probably obtain a better fit to STAR data, which show a remarkably linear decrease of v_2 over most of the centrality range.

Note that the value of v_2 calculated in hydro models depends weakly on the scenario chosen for the longitudinal expansion, which is to a large extent arbitrary.

To summarise, one can make a rather firm statement that thermalisation implies a linear decrease of v_2 with centrality, with a slope that depends (in fact not very strongly) on the equation of state. The centrality dependence of elliptic flow therefore yields valuable information: deviations from a linear decrease can be used to signal a phase transition [12] or a departure from thermal equilibrium [13]. If thermalisation is only partial, departures from thermalisation are expected to be more significant for the more peripheral collisions: the size of the system is smaller, so that particles undergo fewer collisions, and v_2 should be smaller than the hydro prediction. Then, the maximum of v_2 occurs at less peripheral collisions than if thermalisation if fully achieved. This is indeed observed in several specific transport models like UrQMD [14] (which however predicts a much too small value of v_2), QGSM [15], and AMPT [16]. These models contain final state interactions but do not assume perfect thermalisation.

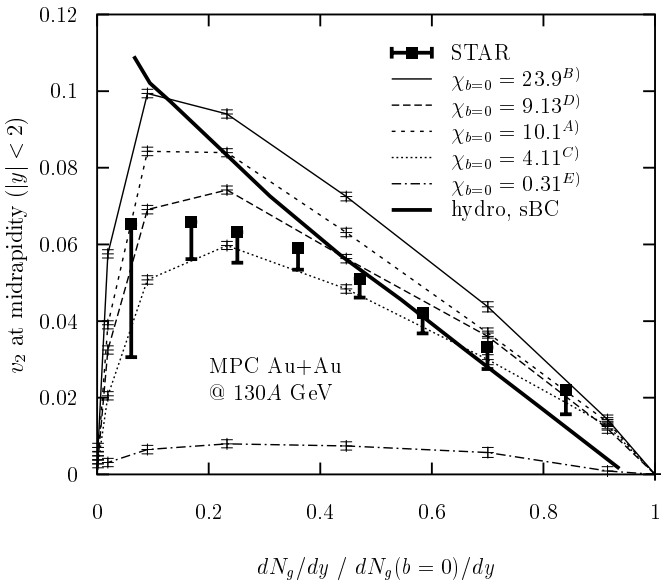

Figure 4. Predictions from a transport calculation. The strength of final state interactions increases from bottom to top. As interactions increase, v_2 increases, and the maximum of v_2 shifts towards more peripheral collisions. From D. Molnar and M. Gyulassy [17].

This modification of the centrality dependence for a partially thermalized system is illustrated in Fig. 4, which displays a systematic study of the variation of v_2 as the strength

of interactions increases [17]. This shows that one can in principle relate the observed centrality dependence of v_2 to the degree of thermalisation of the system. However, it is worth noting that experimental results vary significantly depending on the method used to analyse elliptic flow [1,18]. We come back to this issue in Sec. 3.

2.4 p_T dependence of elliptic flow

Hydrodynamical calculations were also able to predict [19] the p_T dependence of v_2 for identified hadrons, in remarkable agreement with experimental results [20]: v_2 is almost linear in p_T for pions and significantly smaller for protons. This is illustrated in Fig. 5. However, these non-trivial features are also reproduced by transport models [14–16], which do not assume full thermalisation.

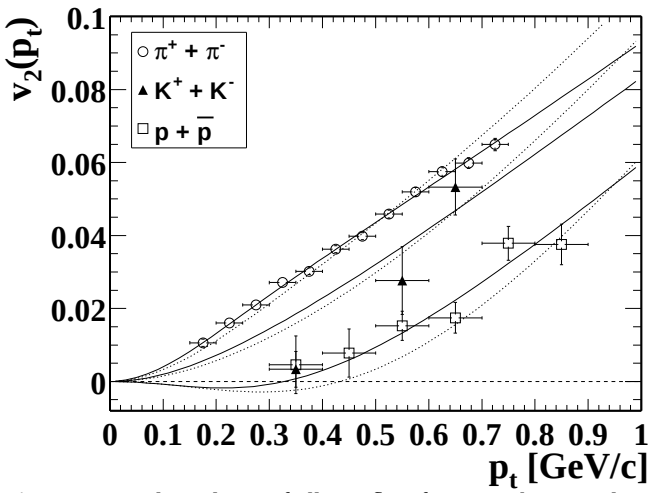

Figure 5. p_T dependence of elliptic flow for pions, kaons and protons, measured by the STAR Collaboration at RHIC, together with predictions from a thermal model, from Ref. [20].

In addition, the latter predict a saturation [17] for p_T above 2 GeV which is not seen in hydrodynamical calculations, suggesting that many elastic collisions are necessary to build the flow at high p_T. This saturation, which is seen in the data [21] has also been proposed as a possible signature of jet quenching [22].

3. Analysing elliptic flow with multiparticle correlations

Measuring elliptic flow, and more generally anisotropic flow, is far from obvious. Indeed, the orientation of the reaction plane is unknown experimentally, so that the azimuthal angle ϕ defined in Fig. 1 is not a measurable quantity. This means that elliptic flow defined by Eq. (2) is not directly measurable. Only *relative* azimuthal angles can be measured experimentally.

3.1 Flow from azimuthal correlations

The standard flow analysis [23] relies on the key assumption that particles are uncorrelated. This allows one to write [24]:

$$\left\langle e^{2i(\phi_1-\phi_2)} \right\rangle = \left\langle e^{2i\phi_1} \right\rangle \left\langle e^{-2i\phi_2} \right\rangle = (v_2)^2, \tag{3}$$

where brackets denote an average over pairs of particles belonging to the same event and we have used the definition of elliptic flow in complex form, Eq. (2). From the measured two-particle average in the left-hand side, one thus obtains the elliptic flow v_2, up to a sign.

One could also use multiparticle observables, such as the following four-particle average:

$$\left\langle e^{2i(\phi_1+\phi_2-\phi_3-\phi_4)} \right\rangle = \left\langle e^{2i\phi_1} \right\rangle \left\langle e^{2i\phi_2} \right\rangle \left\langle e^{-2i\phi_3} \right\rangle \left\langle e^{-2i\phi_4} \right\rangle = (v_2)^4, \tag{4}$$

with ϕ_1, ϕ_2, ϕ_3 and ϕ_4 the angles of particles belonging to the same event. However, such equations are not quite correct, since they neglect correlations between particles, which contribute to the above averages. We call these additional contributions "nonflow correlations". We now estimate the magnitude of nonflow correlations by means of a very simple example, and then discuss to what extent they may bias experimental results.

3.2 Simple illustration of nonflow correlations

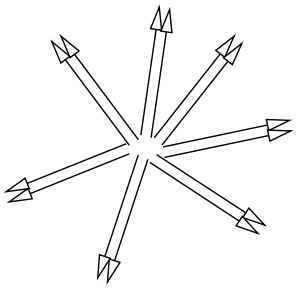

Figure 6. Illustration of nonflow correlations: $M = 14$ particles are produced in $M/2 = 7$ collinear pairs.

In order to illustrate nonflow correlations, we consider the following example: assume that in each event, $M/2$ pairs of particles are emitted, where both particles in a pair have collinear momenta, but pairs are emitted with random orientations (see Fig. 6). Since azimuthal angles of the pairs are randomly distributed, elliptic flow defined in Eq. (2) vanishes. On the other hand, averages in the left-hand sides of Eq. (3) and Eq. (4) do not vanish. In each event, there is a total of $M(M-1)/2$ particle pairs, among which $M/2$ are correlated, hence the two-particle average

$$\left\langle e^{2i(\phi_1-\phi_2)}\right\rangle = \frac{1}{M-1}. \tag{5}$$

A similar reasoning yields the four-particle average:

$$\left\langle e^{2i(\phi_1+\phi_2-\phi_3-\phi_4)}\right\rangle = \frac{2M(M-2)}{M(M-1)(M-2)(M-3)} = \frac{2}{(M-1)(M-3)}. \tag{6}$$

In this case, applying Eqs. (3) or (4) to obtain the flow, one would obtain $v_2 \sim 1/\sqrt{M}$, although there is no flow.

This example is by no means realistic, but does reproduce the correct order of magnitude of nonflow correlations, which in practice arise from various effects such as quantum correlations between identical particles, global momentum conservation, resonance decays [25], etc.

3.3 Why nonflow correlations are important at SPS and RHIC

When flow is present, nonflow correlations produce an *additive* term in the right-hand side of Eq. (3), which becomes

$$\left\langle e^{2i(\phi_1-\phi_2)}\right\rangle = (v_2)^2 + \mathcal{O}(1/M), \tag{7}$$

where the last term is the nonflow contribution, whose order of magnitude is given by Eq. (5). At SPS energies, $M \simeq 2500$ for a central Pb-Pb collision, while v_2 is of the order of 3%: both terms in the right-hand side of Eq. (7) are of the same order, and one may no longer ignore nonflow correlations. Similar arguments apply to directed flow v_1.

One can show more explicitly that nonflow correlations are important at SPS by considering well-known sources of correlations, and estimating their contribution to the last term of Eq. (7). For example, quantum correlations between identical particles (HBT correlations) produce sizeable azimuthal correlations between particles with low relative momenta. Taking this effect into account, one is led to revise significantly the values of the flow given by the standard analysis. This is illustrated in Fig. 7 which shows the corresponding modification in the case of pion directed flow. Accounting for correlations due to global momentum conservation also leads to significant corrections.

At RHIC, both the elliptic flow v_2 and the multiplicity M are higher, so that, following Eq. (7), one may naively expect that nonflow correlations become negligible. However, new effects may appear at RHIC which are not present at SPS, in particular correlations within minijets, which produce a number of almost collinear particles, so that nonflow correlations should also be considered. We shall see in Sec. 3.4 that they are in fact probably significant at RHIC.

Although it is impossible to give an exhaustive list of all physical effects producing nonflow correlations, one can show under very general assumptions that their centrality dependence follows the $1/M$ scaling rule in Eq. (7). As a consequence, nonflow effects are more important for peripheral collisions. In measuring the centrality dependence of v_2, which is crucially important for peripheral collisions as discussed in Sec. 2.3, one must therefore carefully eliminate nonflow correlations.

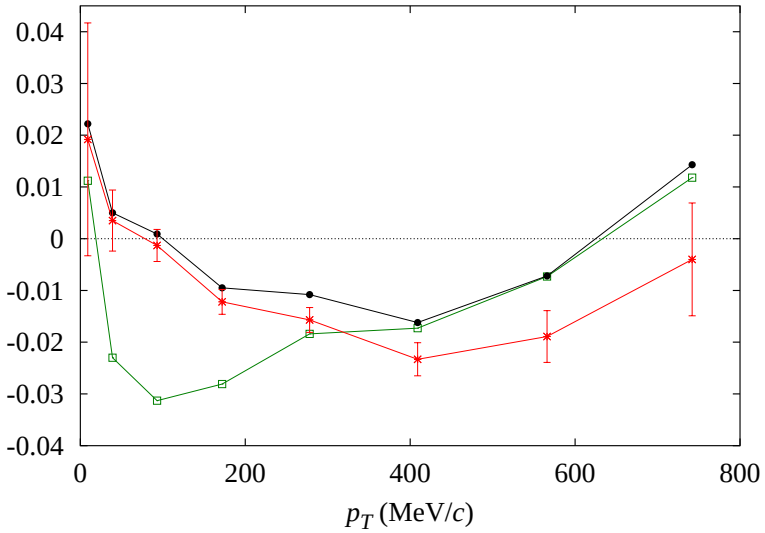

Figure 7. Directed flow of pions in Pb-Pb collisions at 158 GeV per nucleon. Open squares: result of the standard flow analysis performed by NA49 [10]; full squares: after subtraction of HBT correlations; stars: after subtraction of correlations from global momentum conservation (from [25]).

3.4 Systematic elimination of nonflow correlations

Although one cannot estimate quantitatively the magnitude of all nonflow correlations, one can greatly reduce their contribution by combining the informations from two- and four-particle averages, left-hand sides of Eqs. (3) and (4). Indeed, let us assume that particles are pairwise correlated. Then, the four-particle average can be written as a sum of two terms:

$$\left\langle e^{2i(\phi_1+\phi_2-\phi_3-\phi_4)}\right\rangle = \left\langle e^{2i(\phi_1-\phi_3)}\right\rangle\left\langle e^{2i(\phi_2-\phi_4)}\right\rangle + \left\langle e^{2i(\phi_1-\phi_4)}\right\rangle\left\langle e^{2i(\phi_2-\phi_3)}\right\rangle . \tag{8}$$

The first term in the right-hand side corresponds to the situation where particles 1 and 3 form one pair and particles 2 and 4 a second pair, while the second term corresponds to the second possibility, 1 with 4 and 2 with 3 (the third possibility, namely 1 with 2 and 3 with 4, gives a vanishing contribution). If averages are taken over all possible 4-uplets of particles, this equation becomes simply

$$\left\langle e^{2i(\phi_1+\phi_2-\phi_3-\phi_4)}\right\rangle = 2\left\langle e^{2i(\phi_1-\phi_2)}\right\rangle^2 . \tag{9}$$

Now, both sides of this identity are measurable quantities. Subtracting the right-hand side from the left-hand side, one therefore obtains a quantity which vanishes if particles are correlated pairwise. This is the *cumulant* of the four-particle correlation.

Let us illustrate how this works on the simple explicit example discussed in Sec. 3.2. From Eqs. (6) and (5), one obtains the following explicit expression for the cumulant:

$$\left\langle e^{2i(\phi_1+\phi_2-\phi_3-\phi_4)}\right\rangle - 2\left\langle e^{2i(\phi_1-\phi_2)}\right\rangle^2 = \frac{4}{(M-1)^2(M-3)}. \tag{10}$$

It does not strictly vanish although particles are only correlated pairwise, but it is by a factor $1/M$ smaller than the four-particle average (6): most of nonflow correlations are eliminated by taking the cumulant.

Quite remarkably, the cumulant no longer vanishes if elliptic flow is present. It thus yields an estimate of v_2, easily obtained by combining Eqs. (3) and (4):

$$\left\langle e^{2i(\phi_1+\phi_2-\phi_3-\phi_4)}\right\rangle - 2\left\langle e^{2i(\phi_1-\phi_2)}\right\rangle^2 = -(v_2)^4, \tag{11}$$

and this estimate is essentially *free from nonflow correlations* [26].

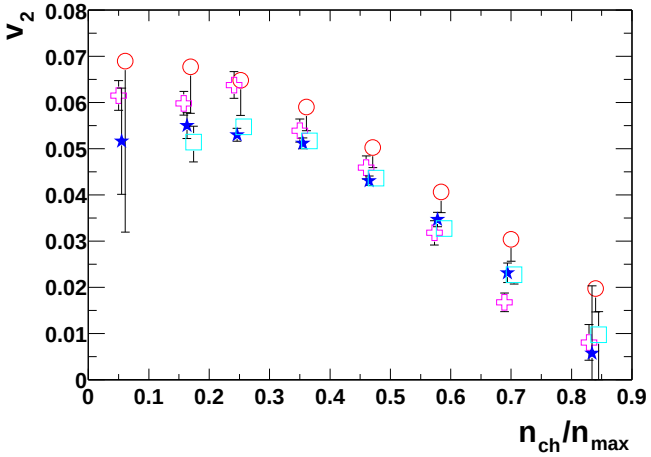

Figure 8. Elliptic flow versus centrality. Circles: from the standard, two-particle analysis; stars: from the cumulant of four-particle correlations (from [27]).

This method was recently applied to STAR data [18,27]. The corresponding centrality dependence of elliptic flow is displayed in Fig. 8. The values of v_2 from cumulants of four-particle correlations are significantly smaller than those obtained with the standard flow analysis, in particular for the most peripheral collisions. This is precisely where nonflow effects are expected to give the largest contribution since the multiplicity M is smaller (see Eq. (7)). The centrality dependence obtained with this method suggests that departures from thermalisation at RHIC may be larger than was previously thought.

The cumulant expansion, which was illustrated above on 4-particle correlations, can be generalized to an arbitrary number of particles [26]. The practical implementation of the method is described in Ref. [28]. Flow, which is essentially a collective phenomenon, contributes to all orders, while the relative contribution of nonflow correlations decreases as the order increases. Higher order cumulants therefore provide a unique possibility to check quantitatively that azimuthal correlations are indeed of collective origin.

Acknowledgments

J.-Y. O. thanks Denes Molnar and Raimond Snellings for discussions.

References

[1] K. H. Ackermann *et al.* [STAR Collaboration], Phys. Rev. Lett. **86**, 402 (2001); R. A. Lacey *et al.* [PHENIX Collaboration], Nucl. Phys. A **698**, 559c (2002); I. C. Park *et al.* [PHOBOS Collaboration], Nucl. Phys. A **698**, 564c (2002).
[2] P. F. Kolb, P. Huovinen, U. W. Heinz and H. Heiselberg, Phys. Lett. B **500**, 232 (2001)
[3] P. Braun-Munzinger, D. Magestro, K. Redlich and J. Stachel, Phys. Lett. B **518**, 41 (2001); F. Becattini, J. Cleymans, A. Keranen, E. Suhonen and K. Redlich, Phys. Rev. C **64**, 024901 (2001).
[4] E. V. Shuryak, Phys. Rev. Lett. **68**, 3270 (1992).
[5] See for instance R. Baier, A. H. Mueller, D. Schiff and D. T. Son, Phys. Lett. B **502**, 51 (2001) and references therein.
[6] J.-Y. Ollitrault, Phys. Rev. D **46**, 229 (1992).
[7] S. Voloshin and Y. Zhang, Z. Phys. C **70**, 665 (1996).
[8] For a short review, see J. Y. Ollitrault, Nucl. Phys. A **638**, 195c (1998).
[9] J. Barrette *et al.* [E877 Collaboration], Phys. Rev. C **56**, 3254 (1997).
[10] H. Appelshäuser *et al.* [NA49 Collaboration], Phys. Rev. Lett. **80**, 4136 (1998).
[11] P. F. Kolb, U. W. Heinz, P. Huovinen, K. J. Eskola and K. Tuominen, Nucl. Phys. A **696**, 197 (2001).
[12] H. Sorge, Phys. Rev. Lett. **82**, 2048 (1999).
[13] S. A. Voloshin and A. M. Poskanzer, Phys. Lett. B **474**, 27 (2000).
[14] M. Bleicher and H. Stöcker, Phys. Lett. B **526**, 309 (2002).
[15] E. E. Zabrodin, C. Fuchs, L. V. Bravina and A. Faessler, Phys. Lett. B **508**, 184 (2001).
[16] Z. w. Lin and C. M. Ko, Phys. Rev. C **65**, 034904 (2002).
[17] D. Molnar and M. Gyulassy, Nucl. Phys. A **697**, 495 (2002) [Erratum-ibid. A **703**, 893 (2002)]. D. Molnar, hep-ph/0111401.
[18] A. H. Tang (STAR Collaboration), hep-ex/0108029.
[19] P. F. Kolb, J. Sollfrank and U. W. Heinz, Phys. Rev. C **62**, 054909 (2000); P. Huovinen *et al.*, Phys. Lett. B **503**, 58 (2001).
[20] C. Adler *et al.* [STAR Collaboration], Phys. Rev. Lett. **87**, 182301 (2001).
[21] R. J. Snellings [STAR Collaboration], Nucl. Phys. A **698**, 193c (2002).
[22] X. N. Wang, Phys. Rev. C **63**, 054902 (2001).
[23] P. Danielewicz and G. Odyniec, Phys. Lett. B **157**, 146 (1985); A. M. Poskanzer and S. A. Voloshin, Phys. Rev. C **58**, 1671 (1998).
[24] S. Wang *et al.*, Phys. Rev. C **44**, 1091 (1991).
[25] P. M. Dinh, N. Borghini and J.-Y. Ollitrault, Phys. Lett. B **477**, 51 (2000); Phys. Rev. C **62**, 034902 (2000).
[26] N. Borghini, P. M. Dinh and J.-Y. Ollitrault, Phys. Rev. C **63**, 054906 (2001); Phys. Rev. C **64**, 054901 (2001).
[27] C. Adler *et al.* [STAR Collaboration], nucl-ex/0206001.
[28] N. Borghini, P. M. Dinh and J.-Y. Ollitrault, nucl-ex/0110016.